

Calcium phosphate ceramics for biomedical applications

D. PREDOI^{*}, R.A. VATASESCU-BALCAN^a, I. PASUK, R. TRUSCA^b, M. COSTACHE^a

National Institute of Materials Physics, P.O. Box. MG 07, 077125, Magurele, Romania,

^aMolecular Biology Center, University of Bucharest, 91-95 Splaiul Independenței, 76201, Bucharest 5, Romania

^bMETAV Research & Development, P.O BOX 22, 020011, 31C.A.Rosetti st.,

Bucharest-2, Romania

Calcium phosphate compounds have been studied for biomedical applications due to chemical and structural similarity to the mineral phase of bone and tooth. The composition, physico-chemical properties, crystal size and morphology of synthetic apatite are extremely sensitive to preparative conditions and sometimes it resulted into non-stoichiometric calcium deficient hydroxyapatite (HAp) powders. The present paper describes the synthesis of calcium phosphate ceramics powders via a sol-gel method. The powders were sintered at 600 and 800°C. X-ray diffraction (XRD), scanning electron microscopy (SEM) and energy-dispersive X-ray spectroscopy (EDXS) were used for characterization and evaluation of the phase composition, morphology and particle size of samples. The functional group of the coatings were analyzed using Fourier transform infrared (FTIR). The XRD analysis revealed a well crystallized HA structure at both temperatures. At 800°C a small amount of CaO (about 0.4 %) was detected. The mean crystallite size, determined from the breadth of the diffraction lines, increases from 30 nm at 600°C to about 110 nm at 800°C. FTIR spectra showed the presence of various PO_4^{3-} and OH⁻ groups present in the powders. Osteoblast cells were used to determine cell proliferation, viability and cytotoxicity after interaction with the prepared bioceramics, by MTT (3-(4,5-Dimethylthiazol-2-yl)-2,5-diphenyltetrazolium bromide, a tetrazole) assay. We note that the viability of HAp-600 starts to decrease after 12h, while the viability of HAp-800 decreases after 6h.

(Received June 25, 2008; accepted June 30, 2008)

Keywords: iron-oxide, calcium phosphate, nanoparticles, osteoblasts cells, biocompatibility

1. Introduction

Calcium phosphate ceramics such as hydroxyapatite $[Ca_{10}(PO_4)_6(OH)_2]$ is one of the most effective biocompatible material and is found to be the major component of the bone. These materials are the most promising implant coating materials for orthopedic and dental applications [1-2] due to their good biocompatibility [3-5]. The superior biocompatibility of calcium phosphates contributed by their compositional resemblance with the bone mineral has allowed them to be used [6-7]. They exhibit considerably improved biological affinity and activity compared to other bio-ceramics such as alumina, zirconia.

Various techniques have been used for prepared the hydroxyapatite (HAp). HAp can be prepared by several synthetic routes which include hydrothermal synthesis [8] sol-gel processes [9], direct precipitation from aqueous solutions [10].

The composition, physico-chemical properties, crystal size and morphology of synthetic apatite are extremely sensitive to preparative conditions and sometimes resulted into non-stoichiometric calcium deficient HAp powders.

Osteoblast cells were used to determine proliferation, viability and cytotoxicity interactions with dextrin coated iron oxide nanoparticles and thin film. The osteoblast cells have been provided from the American Type Culture

Collection (ATCC) Center. The outcome of this study demonstrated the effectiveness of bioceramics as a possible non-toxic agent for biomedical applications.

The present paper describes the sol-gel synthesis of hydroxyapatite (HAp), the physical-chemical properties and biocompatibility of HAp after calcinations at 600 and 800°C. The effect of heat treatment on Ca/P ratio and phase content were investigated by EDXS and XRD. The powders were characterized by Fourier transform infrared spectroscopy (FTIR) and scanning electron microscopy (SEM).

2. Experimental

2.1. Powder preparation

The HAp ceramic powder was prepared (Ca/P molar ratio: 1, 67) using $Ca(NO_3)_2 \cdot 4H_2O$ and P_2O_5 by a simple sol-gel approach. A designed amount of phosphoric pentoxide (P_2O_5 , Merck) was dissolved in absolute ethanol to form a 0.5 mol/l solution. A designed amount of calcium nitrate tetrahydrate was also dissolved in absolute ethanol to form a 1.67 mol/l solution [11]. The mixture was stirred constantly for 24 h by a mechanical stirrer, allowing the reaction to complete at ambient temperature. A transparent gel was obtained. The gel was dried at 80°C for 24h in an electrical air oven. The dried gels were individually heated at a rate of 5°C/min up to 600°C (HAp-

600) and 800 °C (HAp-800). The sintered powders were ball milled at 100 rpm to get fine powders.

2.2. Powder characterization

The samples were characterized for phase content by X-ray diffraction (XRD) with a Bruker D8-Advance X-ray diffractometer in the scanning range $2\theta = 20 - 70$ using $\text{CuK}_{\alpha 1}$ incident radiation monochromatized with a Ge(220) double monochromator. An estimation of crystallite sizes was done from the width of the diffraction lines using the Scherrer formula.

The structure and morphology of the samples were studied using a HITACHI S2600N-type scanning electron microscope (SEM), operating at 25kV in vacuum. The SEM studies were performed on powder samples. For the elemental analysis the electron microscope was equipped with an energy dispersive X-ray attachment (EDAX/2001 device).

The functional groups present in the prepared powder and in the powders calcined at different temperatures were identified by FTIR (Spectrum BX Spectrometer). For this 1% of the powder was mixed and ground with 99% KBr. Tablets of 10 mm diameter for FTIR measurements were prepared by pressing the powder mixture at a load of 5 tons for 2 min and the spectrum was taken in the range of 400 to 4000 cm^{-1} with resolution 4 and 128 times scanning.

The thermal behavior of the powders was studied by differential thermal analysis (DTA) and thermal gravimetric analysis (TGA) using a Shimatzu DTG-TA-50 and DTA 50 analyzer in the 25-800 °C temperature range, air environment, and Al_2O_3 reference.

hFOB 1.19 osteoblast cell line used to determine proliferation, viability and citotoxicity interaction with bioceramics have been achieved from the bone of foetus. This line was established by transfection of limb tissue obtained from a spontaneous miscarriage with temperature sensitive expression vector pUCSVtsA58 and neomycin resistance expression vector pSV2-neo. Clones were selected in the presence of 0.6 mg/ml G418. The cells grown at a permissive temperature of 33.5°C exhibit rapid cell division, whereas little or no cell division occurs at a restrictive temperature of 39.5°C. The cells have the ability to differentiate into mature osteoblasts expressing the normal osteoblast phenotype. At the restrictive temperatures, cell division is slowed, differentiation increases, and a more mature osteoblast phenotype is produced. The cells provide a homogenous, rapidly proliferating model system for studying normal human osteoblast differentiation, osteoblast physiology, and hormonal, growth factor, and other cytokine effects on osteoblast function and differentiation.

The cell culture was frozen and stored in liquid nitrogen phase. The vials were thawed rapidly (approximately 2 minutes) by gentle agitation in a 37°C water bath. Subsequent the vial content was transferred to a centrifuge tube containing 9 ml complete culture medium and spin at approximately 1500 rpm for 10 minutes. The pellet was resuspended with the DMEM without phenol red and Ham's F12 medium and dispensed into a 25 cm^2 culture flask. The cells were incubated at 34°C and 5% CO_2 in air atmosphere. The flask was seeded with cells grown and completely filled with medium at

ATCC to prevent loss of cells during shipping (ATCC Catalog No. CRL-11372, Cell Line Designation hFOB 1.19, osteoblast human).

These cells were further grown in a medium containing a 1:1 mixture of Dulbecco's Modified Eagle's Medium (DMEM) without phenol red and Ham's F12 medium with 2.5 mM L-glutamine adjusted to contain 15 mM HEPES, 0.5 mM sodium pyruvate, 1.2 g/L sodium bicarbonate and supplemented with 0.3 mg/ml G418, 10% fetal bovine serum. This medium is formulated for use with a 5% CO_2 in air atmosphere.

The osteoblasts were suitable for split in flasks after 3-4 days. The subculture was performed at confluence (2,4 x 10⁶ cells/plate) in about 4 days, with a 1:4 ratio. Confluent cultures have been treated with trypsin for 5-15 min and then centrifuged at 1.500 rpm for 10 min. Cells were re-suspended in DMEM without phenol red and Ham's F12 medium volume, counted with Burker-Turk chamber and evenly distributed on sterile supports, previously treated with polylysine.

After osteoblast culture achievement, the cells were treated with 0.25% (w/v) Trypsin 0.03% (w/v) EDTA solution to flask and subcultured in 35/35 mm Petri dishes. Cells were seeded at the same density as previously (10⁴ cells/ml) in Petri dish and incubated on bioceramics for 6, 12 and 24 hours. The cell viability was determined by MTT (3-(4,5-dimethylthiazol-2-yl)-2,5-diphenyltetrazolium bromide) reduction test. The cells were incubated (5% CO_2 atmosphere, T=34°C) for 4h with MTT (0.1 mg/ml). The viability cell number is directly proportional to the production of formazan [12-13]. The isopropanol was added to dissolve the insoluble purple formazan product into a colored solution. The absorbance at 595 nm (DO₅₉₅) was measured with a TECAN spectrophotometer.

3. Results and discussion

The XRD patterns of HAp-600 and HAp-800 are shown in Fig. 1. Practically all the lines in the patterns belong to hydroxiapatite except several very weak ones originating from CaO. The effect of sintering temperature on the formation plays an important role on the formation on HAp [11]. As the sintering temperature is increased from 600 to 800 °C the HAp peaks become narrower, which suggest an increase in the crystallite size. The mean crystalline size was determined using the Scherrer formula:

$$D_{\text{crystallite}} = K\lambda/B_r \cos\theta$$

where λ is the wavelength of the X-ray, θ is the Bragg angle, K is a constant (0.9), B_r is the line broadening due to crystallite size. The analysis was performed on the basis the full width at half maximum of the (222) reflection of HAp ($2\theta \approx 46.7^\circ$). A corundum reference sample (NIST SRM 1976) was used in order to correct for the instrumental line width. We assumed that the whole line broadening of HAp is due to the small crystallite size (strain broadening neglected). With this rough approximation we obtained $D \approx 35(\pm 5)$ nm at 600 °C and $D = 110(\pm 20)$ nm at 800 °C

A very small amount of CaO was identified in the powder treated at 800 °C. The concentration of CaO is around 0.4 wt % as obtained by Rietveld quantitative phase analysis. In the pattern of HAp 600 °C CaO is below the sensitivity limit of the method. With the increase of the calcination temperature HAp would have started losing hydroxyl groups forming various phosphates. This is in agreement with those reported earlier by Kutty [15] and Skinner et al [16]. The proposed reaction is [11]:

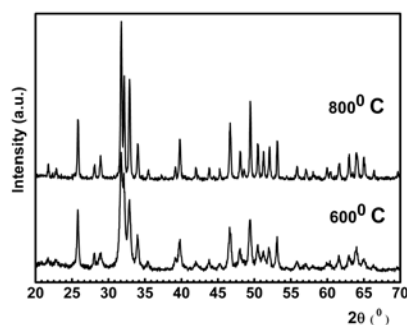


Fig. 1. The X-ray diffraction patterns of the powder after heat treatment at 600°C (sample 1) and 800°C (sample 2).

The decomposition temperature strongly depends on the synthesis technique of the HAp powder. The TGA and DTA curves of the hydroxyapatite dried at 80°C are shown in Figure 2. Weight losses were about 3.12 and 5.84 %, for temperatures from 25 and 1300°C. A relatively pronounced mass loss occurs between 25 and 600°C, with the associated endothermic peak attributed to adsorbed water. From 800°C to 1300°C, a slight decrease in TGA curves shows the decomposition of $\text{Ca}_{10}(\text{PO}_4)_6$ in $\text{Ca}_3(\text{PO}_4)_2$ and CaO.

Fig. 3 shows the SEM micrographs of the powder obtained after heat-treatment at 600 and 800°C. Figure 2a shows a homogeneous microstructure. Figure 2b progresses more rapidly to form a microstructure with nearly equiaxed grains.

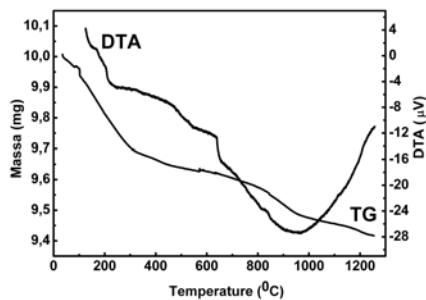


Fig. 2. DTA and TG curves of the gel dried at 80°C (trace at a heating rate of 10 °C/min in air).

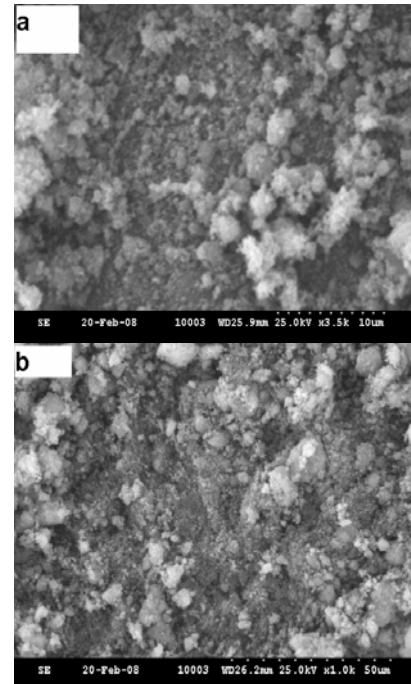


Fig. 3. Typical SEM images of the powders obtained after heat-treatment at 600°C (a) and 800°C (b).

Fig. 4 is representative of the FT-IR spectra of the HAp at room temperature and heated at 600 and 800°C. The bands at 570 cm⁻¹ and 600 cm⁻¹ were assigned to the O-P-O bending mode (ν_3). The absorption bands of P-O, due to PO_4^{3-} groups, in the 1200-1000 cm⁻¹ region, are characteristic to HAp while the absorption band of O-H-O at 1600 cm⁻¹ is due to the absorbed water.

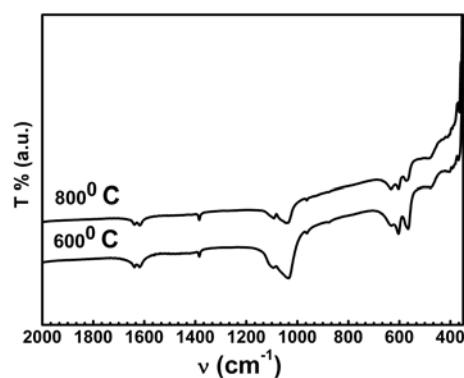


Fig. 4. The FT-IR spectra of powder obtained after heat-treatment at 600°C (HAp-600) and 800°C (HAp-800).

Osteoblast cells were permanent monitored to detect any possible influence due to bioceramics that might modify the cell growth, viability and proliferation. Electronic microscopy was used, but we observed no obvious alteration in HAp-600 and HAp-800 substrates comparative to the control; cells displayed normal fenotypes (Figs. 5, 6).

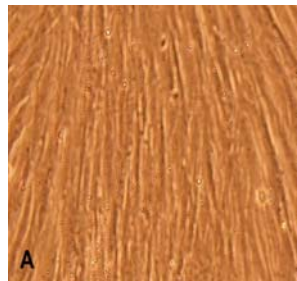


Fig. 5. Phase contrast micrographs in for hFOB 1.19 osteoblasts (objective 20x): A, B-control.

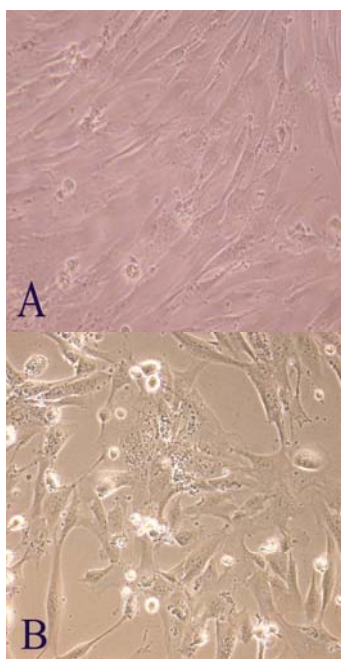


Fig. 6. Phase contrast micrographs for hFOB 1.19 osteoblasts (objective 10x): A - HAp-600 and B - HAp-800.

MTT assay is a standard colorimetric test for measuring cellular proliferation and cell growth. It is used to determine cytotoxicity of potential medicinal agents and other toxic materials.

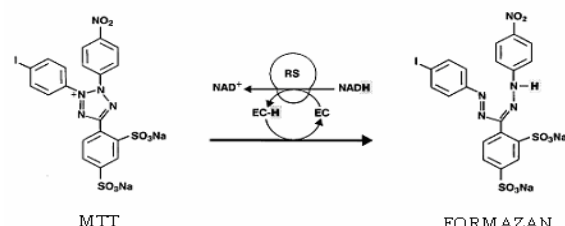


Fig. 7. MTT is reduced to formazan in mitochondria of the cells.

Yellow MTT is reduced to purple formazan in the mitochondria of living cells (Figure 7). A solubilization solution (isopropanol) is added to dissolve the insoluble purple formazan product into a colored solution. The absorbance of this colored solution can be quantified by measuring at a certain wavelength (usually between 500 and 600 nm) by a spectrophotometer. This reduction takes place only when mitochondrial reductase enzymes are active, and therefore the conversion is directly related to the number of viable cells. When the amount of purple formazan produced by cells treated with an agent is compared with the amount of formazan produced by untreated control cells, the effectiveness of the agent in causing death of cells can be deduced, through the production of a dose-response curve. This study represents one of the key-step in cell biology, mitochondrial dehydrogenases being essential.

The results obtained after MTT assay have revealed that the absorbance of the control sample is the lowest one (0.108), compared to the preared samples (Table 1). These values are related to the intensity of the colour (deep purple) due to the amount of formazan produced by cells. The higher is the colour intensity the higher is the formazan, concentration and so the biocompatibility of the sample.

Table 1. Absorbance at 595 nm.

Samples	DO _{595nm}	Viability (%)
Control	0.108	100
HAp-600 – 6h	0.109	100.7
HAp-800 – 6h	0.157	144.8
HAp-600 – 12h	0.115	105.6
HAp-800 – 12h	0.147	136.4
HAp-600 – 24h	0.1	92.4
HAp-800 – 24h	0.128	117.8

Compared to the control cells (100%) 6 hours incubation in the presence of the HAp substrates (Table 1), leads to an increase of viability up to 100.7% for HAp-600 and up to 144.8% for HAp-800. After 12 hours osteoblasts exposure the viability of HAp-600 increased to 105.6%, while the viability of HAp-800 was 136.4%. Cells' incubation for 24 hours showed a decrease of the viability for both samples (92.4% for HAp-600 and 117.8% for HAp-800).

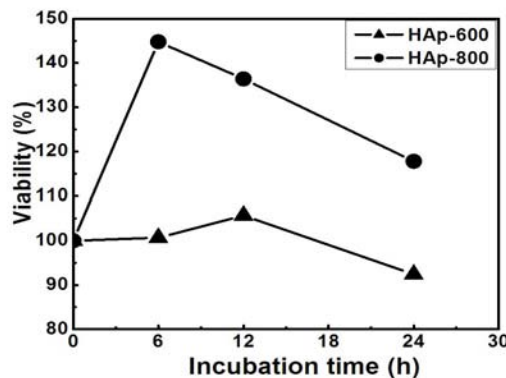


Fig. 8. MTT assay in osteoblast cells growing on HAp-600 and HAp-800 relative to control (100%).

4. Conclusions

The sol-gel method provides a simple route for synthesis of hydroxyapatite nanopowder. The crystalline degree and morphology of the obtained nanopowder depend on the sintering temperature.

The substrates made by the two bioceramics (HAp-600 and HAp-800), could be suitable supports for osteoblasts proliferation without any modification of cell structure and function. The results we obtained using MTT test demonstrate that cells' growing on HAp-600 and HAp-800 bioceramics can modify the growth parameters, leading to a relative modification regarding proliferation and viability, comparing to the control one.

The viability test showed that the incubation time dependence is better for HAp-600 than for HAp-800. One can notice an increase of the viability compared to the control cells (100%) for both samples for incubation time up to 6 h. The viability of HAp-600 starts to decrease after 12 h, while the viability of HAp-800 diminishes progressively after 6 h until 24 h.

It is important to conclude that the structure of hydroxyapatite obtained by the sol-gel method allow them to be used for medical biocompatible supports.

Acknowledgement

This work was financially supported by Science and Technology Ministry of Romania (Project CEEEX_24/2005 and the Project CEEEX_150/2006 VIASAN Program and PNCDI II 71-097/2007).

References

- [1] J. Breme, Y. Zho, L. Groh, *Biomaterials* **16**, 239 (1995).
- [2] N.H.F. Wilson, I.A.J. Mjor, *J. Dent.* **28**, 15 (2000).
- [3] S. Ozawa, S. Kasugai, *Biomaterials* **17**, 23 (1996).
- [4] C. Battistoni, M.P. Casaleotto, G.M. Ingo, S. Kaciulis, G. Mattongo, L. Pandolfi, *Surf. Interface Anal.* **29**, 773 (2000).
- [5] B. Demri, M. Hage-Ali, M. Moritz, J.L. Kahn, D. Muster, *Appl. Surf. Sci.* **108**, 245 (1997).
- [6] L.L. Hench, *ASM*, **4** (1991) 1007.
- [7] H. Aoki, "Science and medical applications of hydroxyapatite, Tokyo, Takayama Press System Centre, JAAS, Tokyo, p.165, 1991.
- [8] M. Yoshimura, H. Suda, K. Okamoto, *J. Mater. Sci.* **29**, 3399 (1994).
- [9] W.J. Weng, J.L. Baptista, *Biomaterials*, **19**, 125 (1998).
- [10] A. Lopez-Macipe, R. Rodriguez-Clemente, A. Hidalgo-Lopez, I. Arita, M.V. Garcia-Garduno, E. Rivera, V.M. Castano, *J. Mater. Synth. Process.* **6**, 121 (1998).
- [11] M. H. Fathi, A. Hanifi, *Materials letters* **61**, 3978 (2007).
- [12] JCPDS Card No 9-432, 1994
- [13] T.R.N. Kutty, *Indian J. Chem.* **11**, 695 (1973).
- [14] H.C.W. Skinner, J.S. Kittelbergen, R.A. Beebe, *J. Phys. Chem.* **79**, 2017 (1975).

*Corresponding author: dpredoi@infim.ro